Applications of Pulsed-Gradient Spin-Echo (PGSE) Diffusion Measurements in Organometallic Chemistry

by **Massimiliano Valentini**, **Heinz Rüegger**, and **Paul S. Pregosin***

Laboratory of Inorganic Chemistry, ETH, Hönggerberg, CH-8093 Zürich

With personal pleasure, we dedicate this 'Perspective' to the memory of *Luigi M. Venanzi*, who, apart from his many scientific contributions, was a major promotor of NMR spectroscopy within the Swiss and international Inorganic Chemistry communities.

Diffusion data from pulsed-field gradient spin-echo (PGSE) methods are shown to be qualitatively useful in the investigation of problems involving unknown molecular aggregation and/or the nature of inter-ionic interactions in metal complexes. For charged species possessing anions such as PF_6^-, BF_4^-, $CF_3SO_3^-$ or $BArF^-$, *both* ^{19}F- and ^1H-PGSE methods offer a valid alternative and, sometimes, unique view of gross and subtle solution molecular structure and dynamics. Problems associated with solvents, concentration, and reproducibility are discussed.

1. Introduction. – Although organometallic chemistry (and especially homogeneous catalysis) continues to move from strength to strength [1–5], the applications of modern NMR methods in these areas have lagged somewhat behind. Slowly, but surely, three-dimensional structures are being solved with NOE- and ROE-NMR methods [6–9]; nevertheless, there are areas, *e.g.*, determining molecular size, aggregation, and/or the nature of interionic interactions, where NMR spectroscopic possibilities have not been sufficiently explored.

A promising NMR method involves the use of pulsed-field gradient spin-echo (PGSE) experiments [10], which can measure the diffusion coefficients of molecules and thus provide information on particle size. PGSE Methods were introduced in 1965 by *Stejskal* and co-workers [11][12] and, since then, have been widely used. In the 1970's, this approach was used to determine diffusion coefficients of organic molecules [13]. In the following decade, variants of this technique have been applied to problems in polymer chemistry [14]. Recently, diffusion data on dendrimers [15–20] and peptides [21–24] as well as on molecules in various environments, *e.g.*, in porous silica [25], and zeolites [26], have been obtained. However, there are very few applications of PGSE methods in coordination and/or organometallic chemistry [27–35].

In an interesting and recent application, *Beck et al.* [27] have studied the polymerization catalyst precursors **1**–**5**. Their results prompted the authors to suggest that these zirconium complexes can exist as ion-quadruples in the presence of a boron-based cocatalyst. In their construction of novel Pt-molecules, *Olenyuk et al.* [28] employed diffusion data to support a self-assembled dodecahedron structure of the product of the reaction shown in the *Scheme*. In a bio-inorganic application, *Gorman et al.* [15] estimated the hydrodynamic radii of the iron-sulphur based dendrimers, abbreviated below, using PGSE studies. These three examples are impressive as much for their scarcity as for their elegance.

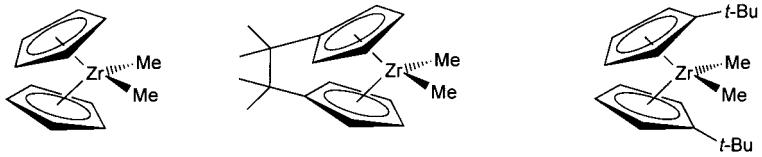

1 **2** **3**

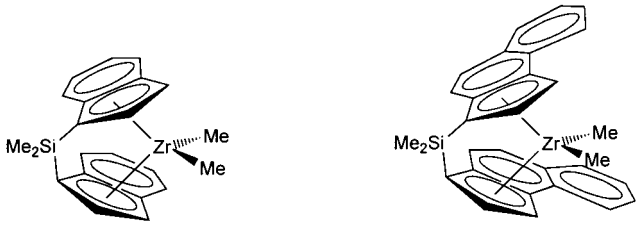

4 **5**

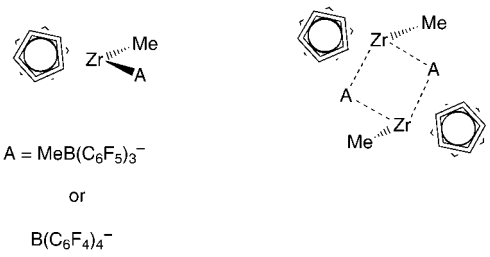

Scheme

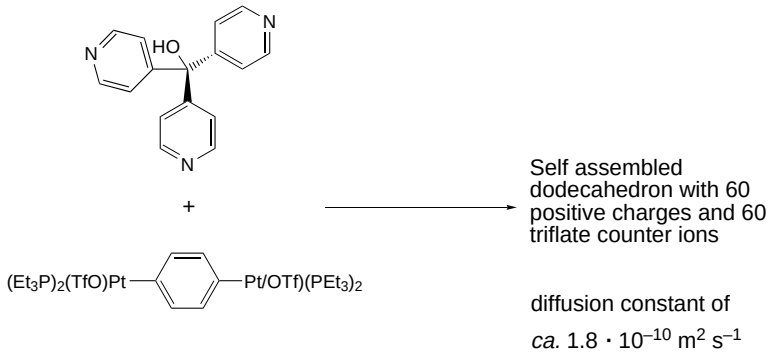

Parallel to the few studies noted above, we have been applying PGSE measurements to a variety of problems in coordination and organometallic chemistry [30][31][34][35]. As we shall show, this method provides a valid alternative to esti-

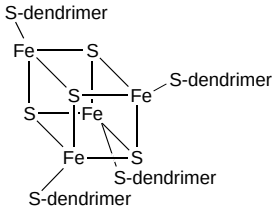

mating molecular volumes (*via* either mass spectroscopic [36] or colligative methods [37]) and provides a unique approach to ion pairing and ion association in metal complexes.

2. Methodology. The basic element of an NMR diffusion measurement consists of a spin-echo sequence, in combination with the application of static- or pulsed-field gradients [10][38][39]. Several common sequences are shown in *Fig. 1*. In the *Stejskal-Tanner* experiment, *Fig. 1,a*, transverse magnetization is generated by the initial $\pi/2$

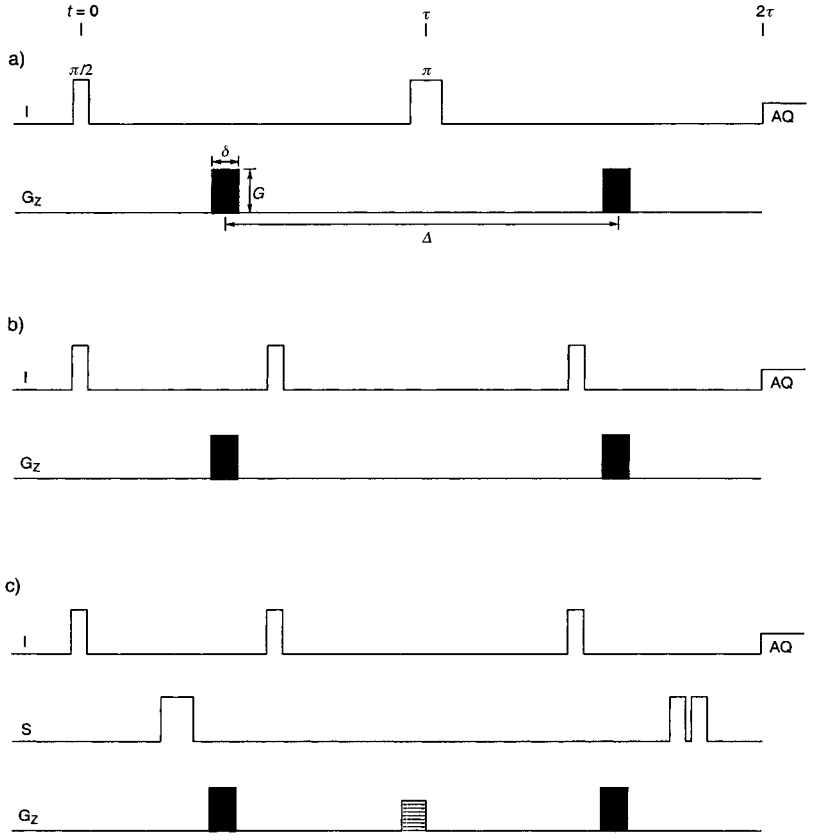

Fig. 1. *Pulse sequences used for the PGSE measurements*

pulse, which, in the absence of the static- or pulsed-field gradients, dephases due to chemical-shift and hetero- and homonuclear-coupling evolution, and spin-spin (T_2) relaxation. After application of an intermediate π pulse at $t=\tau$, the magnetization refocuses, generating an echo at $t=2\tau$. At this point, the sampling (signal-intensity measurement) of the echo decay starts. *Fourier* transformation of these data results in a conventional NMR spectrum, in which the signal amplitudes are weighted by their individual T_2, and the signal phases of the multiplets are distorted by the product $2\,J\tau\pi$. Both effects are present in the diffusion experiment; however, due to the fixed timing, these are kept constant within the experiment.

The application of the first pulsed-linear-field gradient at time τ ($0 < t < \tau$) results in an additional (strong) dephasing of the magnetization with a phase angle proportional to the length (δ) and the amplitude (G) of the gradient. Because the strength of the gradient varies linearly along, *e.g.*, the z-axis, only spins contained within a narrow slice of the sample have the same phase angle. In order words, the spins (and, therefore, the molecules in which they reside) are phase-encoded in one-dimensional space. The second gradient pulse, which must be exactly equal to the first, reverses the respective phases and the echo forms in the usual way. If, however, spins move out of their slice into neighboring slices *via* Brownian motion, the phase they acquire in the refocusing gradient will not be the one they experienced in the preparation step. This leads to incomplete refocusing, as in the T_2 dephasing, and, thus, to an attenuation of the echo amplitude. As smaller molecules move faster, they translate during the time interval Δ into slices that are further apart than in the original, thus giving rise to smaller echo intensities for a given product of δ and G.

Stimulated-Echo Method. The second experiment, shown in *Fig. 1,b*, works quite the same way with the difference that the phase angles encoding the position of the spins are stored along the z-axis in the rotating frame of reference by the action of the second $\pi/2$ pulse. Transverse magnetization and the respective phases are restored by the third $\pi/2$ pulse. This method is advantageous in that, during time Δ, T_1 rather than T_2 is the effective relaxation path. Since T_1 is often longer than T_2, a better signal/noise ratio is obtained. Furthermore, dephasing in multiplets due to homonuclear coupling is attenuated. Technically, both experiments are performed by repeating the sequence while systematically changing either the time allowed for Δ, δ, or G. We routinely use the latter approach with high quality data, which is usually obtained in less than 2 h. The pulse sequence in *Fig. 1,c* will be discussed in connection with the analysis of mixtures.

Mathematically, the diffusion part of the echo-amplitude can be expressed by *Eqn. 1:*

$$\ln\left(\frac{I}{I_0}\right) = -(\gamma\delta)^2 G^2 \left(\Delta - \frac{\delta}{3}\right) D \qquad (1)$$

where, G is the gradient strength, Δ is the delay between the midpoints of the gradients, D is the diffusion coefficient, and δ is the gradient length. The diffusion coefficient D, which is proportional to the slope of the regression line, is obtained by plotting $\ln(I/I_0)$ (I/I_o is the observed spin-echo intensity/intensity without gradients) *vs.* either Δ, δ^2 ($\Delta - \delta/3$) or G^2, and can be related to the hydrodynamic radius of the molecules *via* the *Stokes-Einstein* equation (*Eqn. 2*).

$$D = \frac{kT}{6\pi\eta r_H} \quad (2)$$

where k is the *Boltzmann* constant, T is the absolute temperature, η is the viscosity, and r_H is the hydrodynamic radius. Although the slope and D differ only by a proportionality factor equal to $-(\gamma\delta)^2(\Delta - \delta/3)$, we will report only values of D (and r_H) but not slopes, since the latter have no physical meaning. However, in discussing the data, we often mention the slopes as their significance is easy to visualize. Compounds with larger D move faster, possess smaller r_H, and reveal steeper slopes.

3. Background Studies. – The compounds **6**–**38** form part of our small library of PGSE results. *Figs. 2* and *3* demonstrate the potential of ^{1}H-PGSE methods for some of these complexes. In *Fig. 2*, PGSE results (from left to right) for H_2O, $CHCl_3$, and four arsine complexes of Pd(II), $PdCl_2L_2$, ($L = AsMe_xPh_{3-x}$, $x = 3, 2, 1, 0$), [40] are reported. One can see that the smaller $AsMe_3$ complex moves faster than the analogous $AsMe_2Ph$, which, in turn, is faster than the heavier analogues, and all four of these are slower than H_2O and solvent, which move relatively quickly. This basic point is made even clearer in *Fig. 3*, which gives results for three different ferrocene phosphine dendrimers **18**–**20** [41]. With increasing dendrimer size, one observes decreasing absolute values of the slopes and thus, as shown in *Table 1*, markedly smaller diffusion coefficients and larger hydrodynamic radii.

Table 1. D *and* r_H *Values for* **18**–**20**

Compound	10^{10} D[a]) [m^2 s^{-1}]	r_H[b]) [Å]
18	4.67 (6)[c])	8.4 (1)[c])
19	2.94 (6)	13.4 (1)
20	1.92 (6)	20.6 (1)

[a]) Estimated with the diffusion coefficient of HDO in D_2O as reference [59]. [b]) Calculated with a viscosity value [50] for $CDCl_3$ equal to $0.55 \cdot 10^{-3}$ kg s^{-1} m^{-1}. [c]) Standard deviation.

Table 2 shows measured values of D and r_H for a series of Pd(II) complexes, **6**–**11**, in chloroform. The data given in *Table 2* were obtained with different values of Δ to show *a*) that we can readily reproduce the D and r_H values and *b*) that there is no time-dependent process in addition to diffusion. This latter point implies that the molecular translation movements in $CDCl_3$ are due only to diffusion and not to other processes, *e.g.*, convection.

To demonstrate the validity of the r_H values reported in the various tables, we compared these values with the radii, $r_{X\text{-}Ray}$, estimated from X-ray structures (see *Table 3*). *Fig. 4* shows a plot of the r_H values from the PGSE measurements *vs.* $r_{X\text{-}ray}$. The agreement is acceptable (perhaps too good given the crude approximations).

In addition to $CDCl_3$, we have also used other solvents, *e.g.* THF. Those solvents having viscosity equal to or larger than that of $CHCl_3$ afford constant values of D despite the variation in Δ. With CH_2Cl_2, a lower viscosity solvent, these coefficients

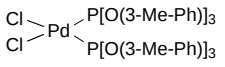

6

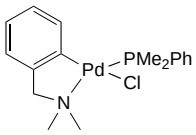

7

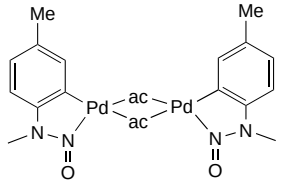

8

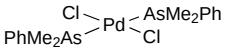

9

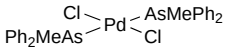

10

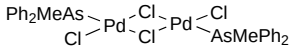

11

12

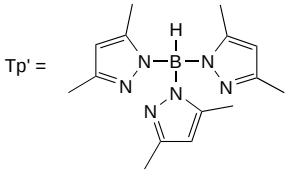

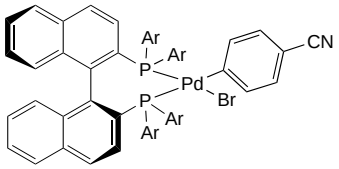

13

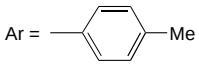

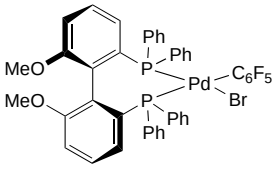

14

$Pd_2(dba)_3$

15

dba =

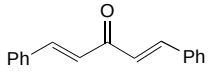

$PdCl_2(AsMe_3)_2$

16

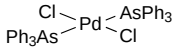

17

were not always constant, perhaps due to convection effects. Nevertheless, we continue to use CH_2Cl_2, but care must be taken with respect to reproducibility. Repeating the experiment with at least 2–3 different Δ values is recommended.

An important subtlety in diffusion studies involves concentration. *Table 4* contains the ^1H diffusion results for $[Pd(\mu\text{-}Cl)Cl(AsMePh_2)]_2$ (**11**) [40] and the Ru-triflate complex **21** [42], each at three different concentrations. For **11**, the diffusion coefficient

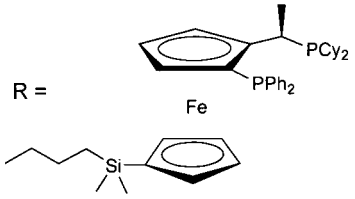

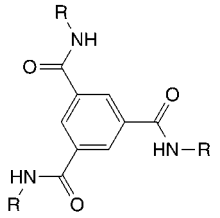

18

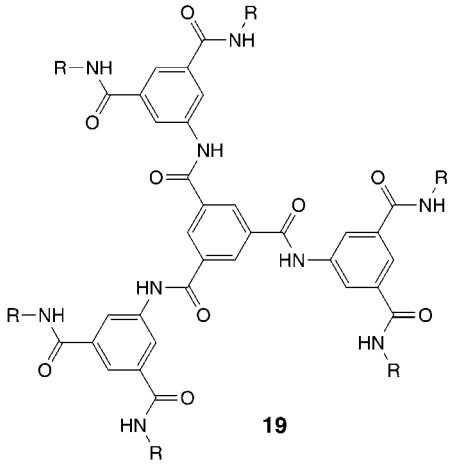

19

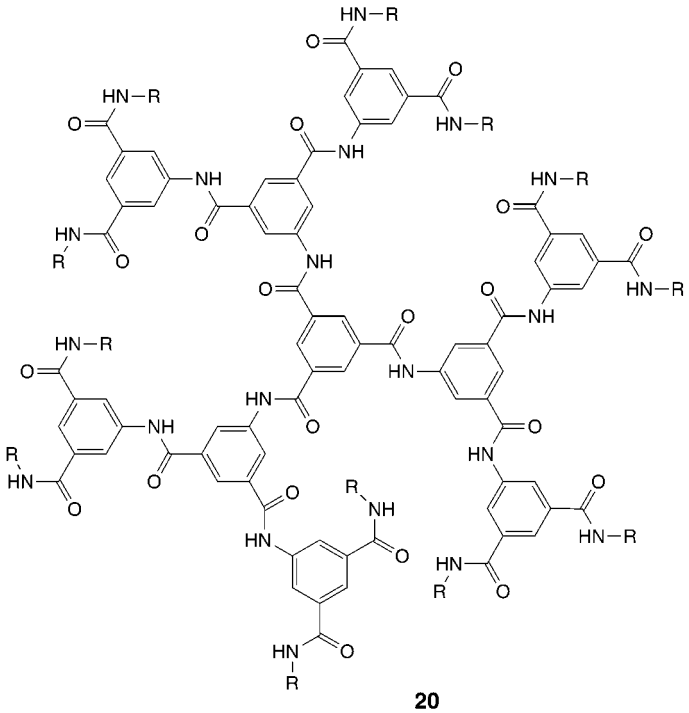

20

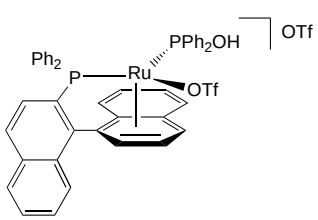

21

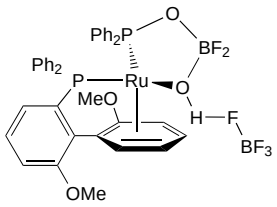

22

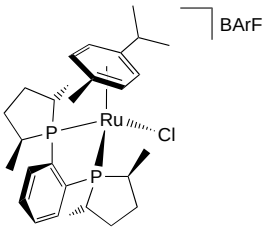

23

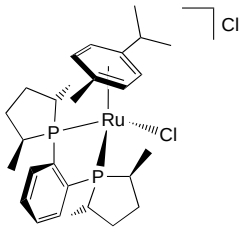

24

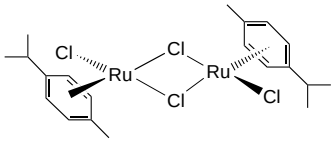

25

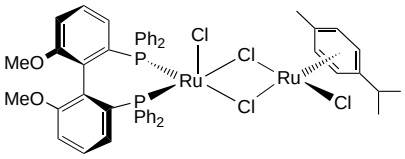

26

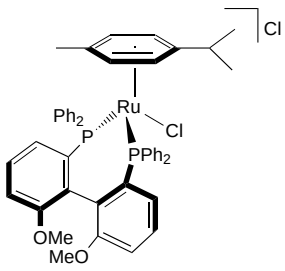

27

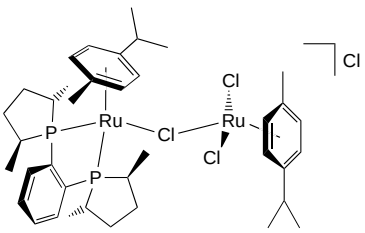

28

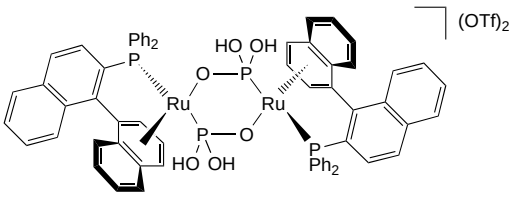

29

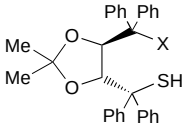

X = OH (**30**), OMe (**31**), NMe_2 (**32**)

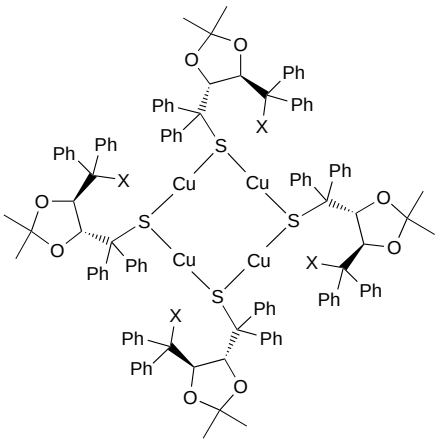

X = OH (**33**), OMe (**34**), NMe_2 (**35**)

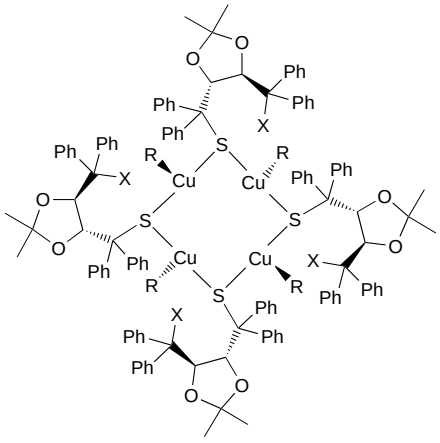

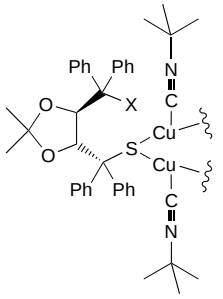

R = $CN(Me)_3$ X = OH (**36**), OMe (**37**), NMe_2 (**38**)

remains constant within the concentration range considered, while, for **21**, it changes by *ca*. 9% and shows the expected higher effective values at lower concentrations[1]). Since changes in D of *ca*. 15–20% indicate almost a doubling of the molecular volume, this concentration effect on D in **21** is relatively large and must be taken into account in order to avoid ambiguous results.

---

[1]) The variation in D is probably due to ion aggregation or to a change in solvent viscosity according to the *Falkenhagen* equation [43][44]. For the viscosity of dilute electrolyte solutions:

$$\eta_{rel} = 1 + A\sqrt{c} \text{ where } A \text{ is: } A = \frac{0.2577\Lambda^{\infty}}{\eta\cdot\lambda_{+}^{\infty}\lambda_{-}^{\infty}\sqrt{\varepsilon T}}\left[1 - 0.6863\left(\frac{\lambda_{+}^{\infty} - \lambda_{-}^{\infty}}{\Lambda^{\infty}}\right)^{2}\right]$$

The term 'A' contains cationic and anionic conductivities at infinite dilution, and 'c' is the concentration. The dependence of the viscosity on the ionic conductivities would explain why there are no changes in D for a neutral compound, while a large variation is observed for charged species.

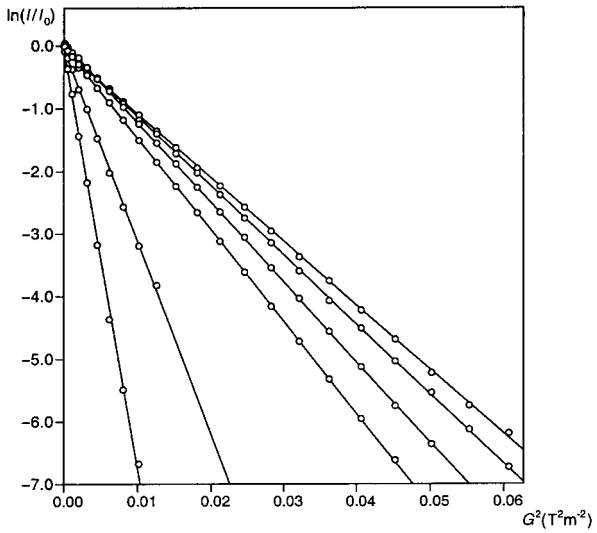

Fig. 2. *Plot of ln* (I/I_o) vs. *the square of the gradient amplitude*. The slopes of the lines are related to the diffusion coefficients, *D*. The six lines stem from H_2O, $CHCl_3$, and the four Pd-arsine complexes $PdCl_2L_2$ (L = $AsMe_xPh_{3-x}$, $x = 3$, 2, 1, 0, increasing molecular volume from left to right). The absolute value of the slope decreases with increasing molecular volume.

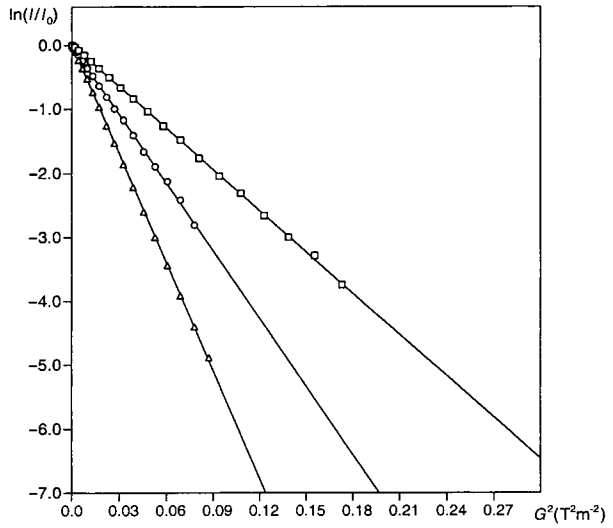

Fig. 3. *Plot of ln* (I/I_o) vs. *the square of the gradient strength for the ferrocene dendrimers* **18**–**20**. The largest compound has the smallest slope and thus the smallest diffusion coefficient.

4. A 'Classical' Application. The Cu(I) thiotaddol chemistry [35] of compounds **30**–**38**, presents a nice opportunity for application of ^{1}H-PGSE methods. The chelating ligands shown as **30**–**32** react with Cu(I) salts to afford the tetranuclear thiolate-bridged Cu(I) complexes, **33**–**35**. These are isolable Cu(I) compounds, and a solid-

Table 2. D *and* r_H *Values for* **6**–**11** *in* $CDCl_3$

6

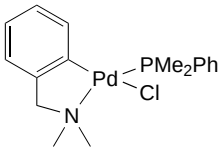

7

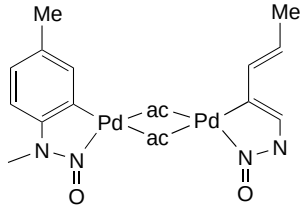

8

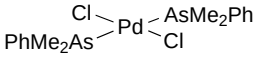

9

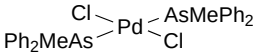

10

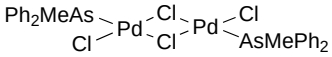

11

Compound	Δ [ms]	10^{10} D [a]) [m^2 s^{-1}]	r_H [b]) [Å]
6	45	6.26 (6)[c])	6.3 (1)[c])
	65	6.21 (6)	6.3 (1)
	85	6.26 (6)	6.3 (1)
7	45	8.41 (6)	4.7 (1)
	65	8.47 (6)	4.7 (1)
	85	8.41 (6)	4.7 (1)
8	65	7.33 (6)	5.4 (1)
	85	7.35 (6)	5.4 (1)
	105	7.37 (6)	5.4 (1)
	125	7.43 (6)	5.4 (1)
9	75	8.37 (6)	4.8 (1)
	85	8.35 (6)	4.8 (1)
	95	8.39 (6)	4.8 (1)
	115	8.27 (6)	4.7 (1)
10	65	7.37 (6)	5.4 (1)
	85	7.41 (6)	5.4 (1)
	95	7.29 (6)	5.3 (1)
	105	7.31 (6)	5.4 (1)
11	65	6.78 (6)	5.8 (1)
	85	6.78 (6)	5.8 (1)
	95	6.82 (6)	5.8 (1)
	105	6.80 (6)	5.8 (1)
	125	6.74 (6)	5.8 (1)

[a]) Estimated with the diffusion coefficient of HDO in D_2O as reference [59]. [b]) Calculated with a viscosity value [50] for $CDCl_3$ equal to $0.55 \cdot 10^{-3}$ kg s^{-1} m^{-1}. [c]) Standard deviation.

state structure has been obtained by X-ray-diffraction methods [35]. Such sulfur-bridged species are interesting since they represent rare examples of chiral chelates functioning as monodentate ligands for a transition metal, and **33**–**35** are catalyst precursors in the enantioselective 1,4-addition of *Grignard* reagents to enones [45]. A

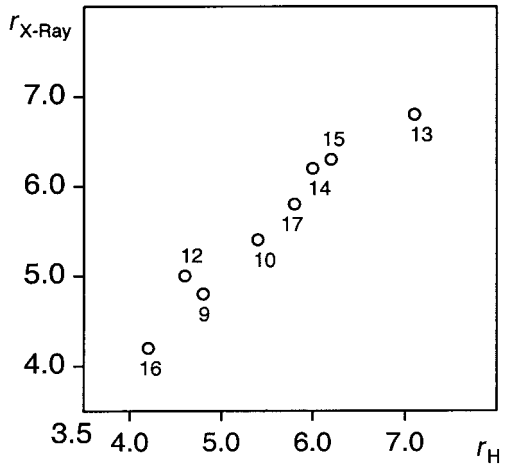

Fig. 4. *Plot of* r_H vs. *the radii calculated from the crystallographic data* (see *Table 3*). For compounds **9**, **10**, **16**, and **17**, the radii in the solid state were estimated on the basis of structures reported for the analogous phosphine instead of arsine.

Table 3. *Estimated Hydrodynamic Radii* r_H [A°]

Compound	Hydrodynamic radius	Radius[a]) from X-ray
9	4.8	4.8[b]) [60]
10	5.4	5.4[c]) [61]
12	4.6	5.0 [62]
13	7.1	6.8 [63]
14	6.0	6.2 [64]
15	6.2	6.3 [65]
16	4.2	4.1[d]) [66]
17	5.8	5.8[e]) [67]

[a]) For compounds **9**, **10**, **16**, and **17** the radii in the solid state were estimated on the basis of reported structures for closely related phosphine, instead of arsine complexes. [b]) *trans*-$PdCl_2(PMeP_2h_2)_2$. [c]) *cis*-$PdCl_2(PMe_2Ph)_2$. *d*) *cis*-$PdCl_2(PMe_3)_2$. [e]) *trans*-$PdCl_2(PPh_3)_2$.

classical problem associated with 'cluster'-catalyst precursors concerns the possibility that the cluster degrades upon addition of substrate. Addition of *tert*-butyl isonitrile to **33**–**35** gives the new and stable complexes, **36**–**38**. The thiolate-bridged derivative **36** maintains its tetra-nuclear character, as shown by PGSE data (see *Fig. 5*). This figure is noteworthy not only for the relatively small slope corresponding to the Cu(I) complex but also for the difference in mobility between the two thiotaddol ligands, **31** and **30**, since for the latter one finds intermolecular H-bonding.

5. Ionic Complexes. – Another typical and informative application of diffusion measurements involves the discrimination between two possible structures, **29** and **39**, *i.e.*, monomeric and dimeric species, for a new complex [46]. The ^{1}H-PGSE diffusion data for this substance and the model compound **21** in CD_2Cl_2 are shown in *Fig. 6*. Very different slopes were found, corresponding to very different diffusion coefficients, for the 'unknown' relative to the model cationic complex. This large difference indicates

Table 4. D *Values for* **11** *and* **21** *in* $CDCl_3$ *at Different Concentrations*

Compound	Concentration [mg/g]	10^{10} D[a]) (m^2 s^{-1})
11	1.3	6.74 (6)[b])
11	7.4	6.82 (6)
11	14.8	6.72 (6)
21	0.8	6.50 (6)
21	6.6	6.12 (6)
21	13.2	5.94 (6)

[a]) Estimated from the diffusion coefficient of HDO in D_2O as reference [59]. [b]) Standard deviation.

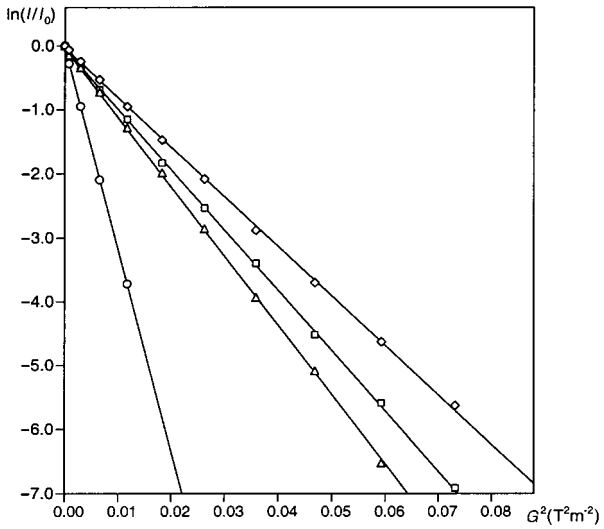

Fig. 5. *Plot of ln* (I/I_o) vs. *the square of the gradient strength for* (left to right) *THF* (○), **31** (△), **30** (□), *and the copper-isocynide complex* **36** (◇) *in* (D_8)*THF solutions*

that the higher-molecular-weight diruthenium complex, **29**, represents the correct structure. The ratio of the D values, *ca*. 1.22, suggests that **29** has *ca*. twice the molecular volume of **21**, since, for two spherical molecules in which one has twice the volume of the other, one expects the ratio of the slopes to be $(2)^{1/3} \approx 1.26$[2]). Model compound **21** and dinuclear **29** are by no means 'innocent', since the counter ion triflate is H-bonded to the P(OH) groups; we shall return to these complexes shortly. Clearly, for both **29** and the copper complex **36**, PGSE data are quite useful.

Until now, our discussion has been focussed primarily on applications of ^{1}H-PGSE results. However, a relatively large number of cationic ruthenium compounds (and palladium and rhodium, *etc.*) are currently in use in homogeneous catalysis and/or organic synthesis. Frequently, these complexes possess anions such as PF_6^-, BF_4^-, $CF_3SO_3^-$ or $BArF^-$. For these, and other complexes, ^{19}F represents both an alternative

[2]) Calculations based on the assumption that the mononuclear complex is spherical and the dinuclear species is elongated with the longer axis twice as long as the smaller, give a ratio of *ca*. 1.18 [47].

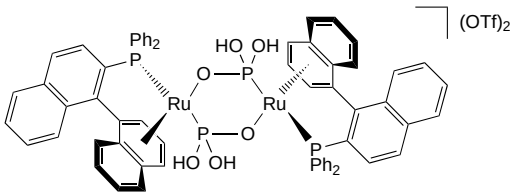

29

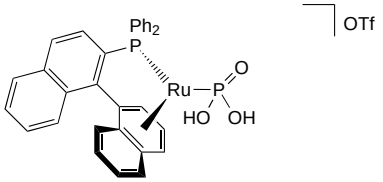

39

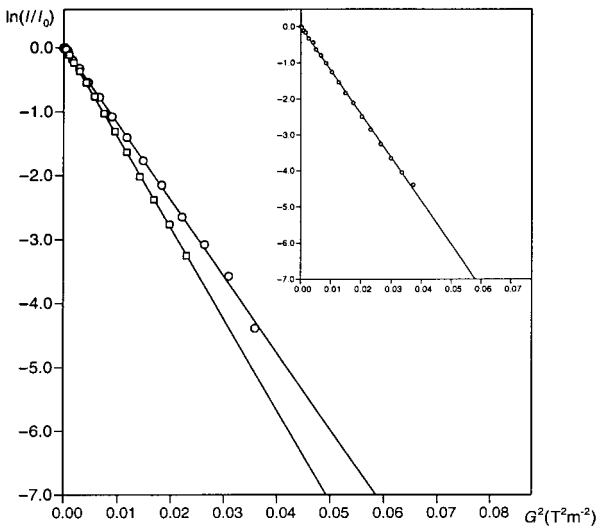

Fig. 6. ^{1}H-PGSE *Results for* **21** (□) *and* **29** (○) *showing markedly different slopes.* The inset shows ^{19}F diffusion results for **29**, which supports that triflate is H-bonded to the P(OH) groups.

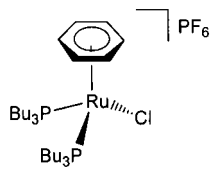

40

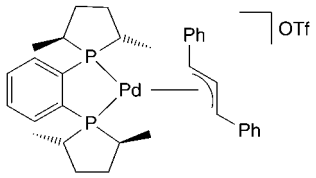

41

and a complement to ^{1}H-PGSE methods. In principle, one can determine the diffusion constants for the cation and anion separately and, thus, investigate ion-pairing.

In this connection, an interesting and unexpected solvent dependence was obtained from PGSE measurements on the ruthenium arene PF_6^- salt **40** [48] and the palladium allyl complex, **41** [49]. *Table 5* shows results in $CDCl_3$ and CD_2Cl_2, for both the cation and the counter-ion (^{1}H and ^{19}F resonances respectively), with *Fig. 7* providing a visual aid. While the two lines for the CD_2Cl_2 solution show different slopes, those in $CDCl_3$

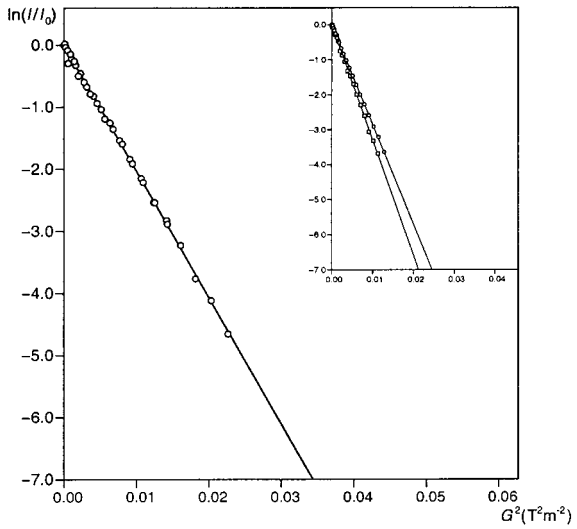

Fig. 7. *Effect of the polarity of the solvent on* **40**. To the left are the two lines (^{1}H and ^{19}F) for **40** in $CDCl_3$, which are strongly overlapped. To the right, in the inset, are the analogous data (^{1}H and ^{19}F) from **40** in CD_2Cl_2. Clearly, in CD_2Cl_2, the cation and anion are diffusing separately. ^{19}F results are corrected for γ_F contributions.

Table 5. D *and* r_H *Values for Cation and Counterion in* $CDCl_3$ *and* CD_2Cl_2 *of* **40** *and* **41**

Compound	Solvent	Fragment	10^{10} D[a]) [m^2 s^{-1}]	r_H[b]) (Å)
40	$CDCl_3$	cation[c])	6.25 (6)[d])	6.3 (1)[d])
	$CDCl_3$	PF_6^- d)	6.27 (6)	6.3 (1)
	CD_2Cl_2	cation[c])	8.74 (6)	6.2 (1)
	CD_2Cl_2	PF_6^-[e])	10.17 (6)	5.3 (1)
41	$CDCl_3$	cation[c])	6.64 (6)	6.0 (1)
	$CDCl_3$	OTf^-[e])	6.45 (6)	6.1 (1)
	CD_2Cl_2	cation[c])	9.14 (6)	5.9 (1)
	CD_2Cl_2	OTf^-[e])	11.69 (6)	4.7 (1)

[a]) Estimated from the diffusion coefficient of HDO in D_2O as reference [59]. [b]) Calculated from viscosity values [50] for $CDCl_3$ and CD_2Cl_2 of $0.55 \cdot 10^{-3}$ and $0.40\ 10^{-3}$ kg s^{-1} m^{-1}, resp. [c]) From ^{1}H signals. [d]) Standard deviation. [e]) From ^{19}F resonance.

are so close that one can barely resolve them. Both complexes exist as tight ion pairs in $CHCl_3$, with the positive fragment and counter-ion revealing the same diffusion coefficients, while, in CH_2Cl_2 solution, the cationic and anionic fragments diffuse at different rates. The dielectric constant and dipole moment for CH_2Cl_2 are both larger than the corresponding values for $CHCl_3$ [50], thus partially rationalizing our observations.

Equally interesting results arise from studies on charged complexes with relatively large anions. On the basis of data collected by the PGSE methodology, *Zuccaccia et al.* [29] recently suggested that the tetraphenyl borate cationic Ru-complexes of pyrazolylmethane **42** [51] (and an analogous pyrazolylborate derivative) can exist as tight ion pairs in dilute $CHCl_3$ solution.

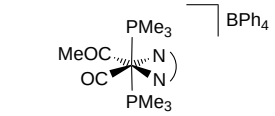

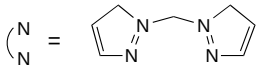

42

The BArF anion is a fluorine-containing derivative of tetraphenyl borate. *Fig. 8* shows ^{1}H-PGSE results for the two Me-duphos compounds **23**, with $BArF^-$, and **24**, with Cl^- [48]. The two slopes, and thus the *D* values (*Table 6*), are quite different, despite the cations being identical. The observed ratio of *D* values, *ca*. 1.21, is consistent with **23** having *ca*. twice the volume of **24**. In the case of **23**, one can rationalize the difference by assuming that the tetraphenyl borate derivative $BArF^-$ in $CDCl_3$ is present as a relatively tight ion-pair (in analogy with **42**), thus effectively doubling the molecular volume. This conclusion is supported by a ^{19}F-PGSE experiment on **23**, which gives a diffusion coefficient for the $BArF^-$ anion almost equal to that found for the cation. Given that there are several known examples of anions that affect results from homogeneously catalyzed reactions [52–54], these PGSE data for complexes such as **23**, and **40**–**42** assume new significance.

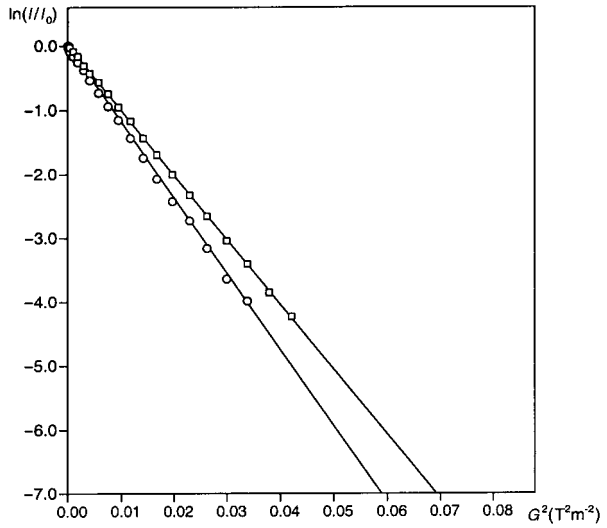

Fig. 8. ^{1}H *Diffusion results for* **23** (□) *and* **24** (○) *in* $CDCl_3$. The slopes for **23** and **24** are quite different despite identical positive fragments. This is due to **23** existing in $CHCl_3$ solution as a tight ion-pair and to the presence of a large counterion, such as $BArF^-$, which almost doubles the molecular volume of **24**.

Table 6. D *and* r_H *values for* **21**–**29**

Compound	Solvent	Nucleus	10^{10} D[a]) [m^2 s^{-1}]	r_H[b]) [Å]
21	$CDCl_3$	^{1}H	6.50 (6)[c])	6.1 (1)[c])
	$CDCl_3$	^{19}F	6.43 (6)	6.1 (1)
	CD_2Cl_2	^{1}H	8.45 (6)	6.1 (1)
23	$CDCl_3$	^{1}H	5.86 (6)	6.7 (1)
	$CDCl_3$	^{19}F	5.66 (6)	7.0 (1)
24	$CDCl_3$	^{1}H	7.09 (6)	5.6 (1)
25	$CDCl_3$	^{1}H	8.37 (6)	4.7 (1)
26	$CDCl_3$	^{1}H	6.43 (6)	6.1 (1)
27	$CDCl_3$	^{1}H	6.19 (6)	6.4 (1)
28	$CDCl_3$	^{1}H	5.70 (6)	6.9 (1)
29	CD_2Cl_2	^{1}H	6.98 (6)	7.4 (1)
	CD_2Cl_2	^{19}F	7.03 (6)	7.3 (1)

[a]) Estimated from the diffusion coefficient of HDO in D_2O as reference [59]. [b]) Calculated from viscosity values for [50] $CDCl_3$ and CD_2Cl_2 of $0.55 \cdot 10^{-3}$ and $0.40 \cdot 10^{-3}$ kg s^{-1} m^{-1} respectively. [c]) Standard deviation.

Yet another promising area concerns H-bonding in metal complexes. *Fig. 9* shows ^{19}F-PGSE data for both triflate moieties of the cationic compound **21**, noted above. The two lines in the figure are so closely overlapped as to be not visibly readily resolved, suggesting that *both* triflates in **21** are moving at the same rate. Although one could imagine tight ion-pairing as an explanation for the observed identical diffusion coefficients, we note that the reported solid-state structure for **21** [42] suggests an H-bond from the $P(OH)Ph_2$ fragment to the anionic (and not to the complexed) triflate. Consequently, the anionic triflate (which might also be involved in ion-pairing) is most likely carried with the cation *via* the OH group. The observed diffusion data from the

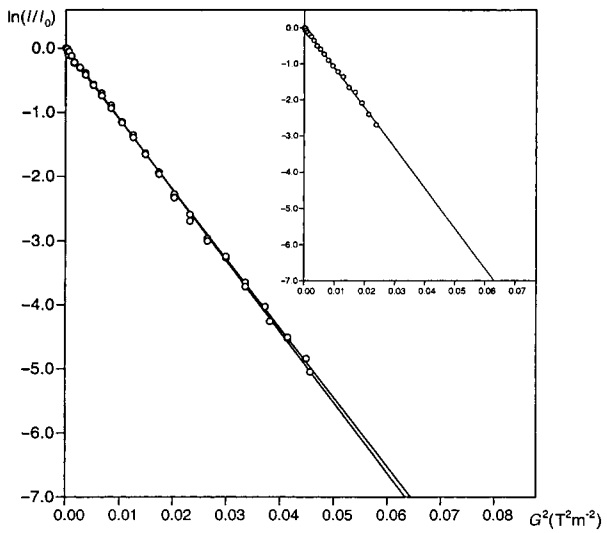

Fig. 9. *Plot of ln (I/I$_0$)* vs. *the square of the gradient strength for* **21** *in* $CDCl_3$ *based on the* ^{19}F *resonance and, in the inset,* ^{1}H *signals.* The slope measured for ^{19}F, corrected for γ_F, is equal to that estimated *via* ^{1}H.

^{19}F study are in excellent agreement with those found from the ^{1}H-PGSE experiment on the protons of the cation.

Interestingly, for **29**, a similar situation exists, *i.e.*, from the ^{19}F diffusion data (see insert in *Fig. 6*), the triflate diffuses at the same rate as the large dication. Again (based on the X-ray data) we assume H-bonding to be important.

Another H-bonding situation exists for the recently reported exotic complex of the Ph_2POBF_2OH bidentate ligand (see **22** [55]). ^{1}H- and ^{19}F-PGSE measurements reveal the same diffusion coefficients for both the complex (*via* the various ^{1}H spins) and the H-bonded BF_4^- (*via* the ^{19}F resonance of the H-bonded BF_4^- unit).

6. Mixtures. ^{1}H-PGSE Experiments provide a collection of responses simultaneously. As long as a molecule has at least one resonance clearly resolved, it is a trivial task to obtain its diffusion coefficient. Mixtures arising from the presence of isomers, diastereomers, impurities, and reference materials are not a problem, and the various diffusion coefficients can be determined from a single experiment.

For relatively complicated chemical systems, it may be necessary to consider a nucleus other than ^{1}H, *e.g.*, ^{19}F or ^{31}P. Alternatively, one can resort to spectral filtering techniques, *e.g.*, T_1 or T_2 relaxation filters [56] or an X-filter [57] with a suitable heteronuclear spin. As the first point is straightforward, and covered in earlier paragraphs, we focus on a relevant filtering technique. Instead of the usual preparation period consisting of a $\pi/2$ pulse, an additional pulse scheme can be added depending on the desired filtering.

Heteronuclear Filters. The application of heteronuclear filters, also called X-filters, has been shown to have the potential to substantially simplify the spectra of complicated systems. The basic idea is simple: only proton spins possessing either scalar or dipolar interactions to a suitable heteronucleus are selected, whereas all the other, more abundant spin-systems, are rejected. With a view to combining PGSE with an X-filter, we have extended the sequence shown in *Fig. 1, b* to that shown in *Fig. 1, c*.

In this sequence, one adds an X-filter element to the end of a diffusion experiment. The potential with respect to diffusion studies is illustrated by a somewhat artificial mixture obtained by mixing the ^{15}N-labelled imine complex of palladium, **43** [58] with an excess of triphenylphosphine, which gives **44**, **45**, and with the arylphosphite complex **6** and 1,1′-binaphthyl (see *Fig. 10*, top). The ^{15}N-filtered spectrum (*Fig. 10*, bottom) shows the prominent features (the imine =CH and the *ortho*-aniline ring spin), as the strong undiminished resonances for **43** as well as **44** and **45**. The attenuation of their amplitudes in the course of the normal PGSE diffusion experiment leads directly to the desired diffusion coefficient of the different complexes. The result for **43** is in excellent agreement with that obtained from a $CDCl_3$ solution of pure **43** obtained by the standard stimulated-echo sequence, D equal to $6.72 \cdot 10^{-10}$ and $6.74 \cdot 10^{-10}$ $m^2\ s^{-1}$ respectively.

7. Comments. – Clearly, whether neutral ferrocene dendrimers or copper thiolate clusters are under consideration, the ability to relatively rapidly estimate the molecular volume of an unknown substance represents a useful addition to our physical armament. Equally interesting, and not at all obvious, is that we can use PGSE data, together with NOESY, HOESY, conductivity, and other physical methods to

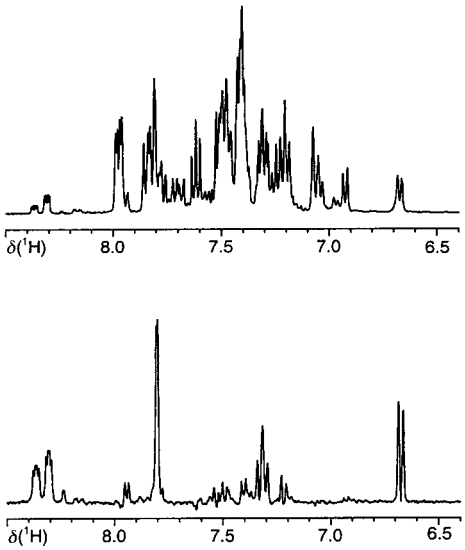

Fig. 10. *Section of the ^{1}H-NMR spectrum of the mixture of 1,1′-binaphthyl*, **6**, *^{15}N enriched* **43**–**45** (top) *and triphenylphosphine and the ^{15}N-filtered spectrum measured with the sequence in* Fig. 1,c *at the minimal gradient strength* (bottom). Note the simplification of the spectrum.

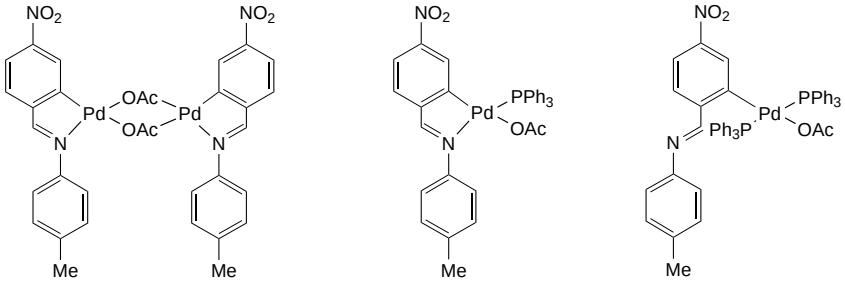

43 **44** **45**

qualitatively investigate problems involving ion-pairing and H-bonding. These last areas pose additional problems (*e.g.*, residence times at one site, simultaneous equilibria, and the exact nature of the ion-pairing, *etc.*) so that the PGSE extension to charged species with complicated structural features is not necessarily trivial; nevertheless, we believe that PGSE methods will open yet another, complementary door into these areas.

In conclusion, we suggest that *both* ^{19}F- and ^{1}H-PGSE methods offer valuable and unique views of gross and subtle solution molecular structure, and that these NMR techniques will find increasing applications in coordination and organometallic chemistry.

P. S. P. thanks the *Swiss National Science Foundation* and the ETH Zürich for financial support. We warmly thank Dr. *K. Selvakumar*, *C. J. den Reijer*, *D. Drago*, and *T. J. Geldbach* for the preparation of most of the complexes studied. We also thank *Johnson Matthey* for the loan of metal salts and *F. Hoffmann-La Roche* for a gift of chemicals.

REFERENCES

[1] E. J. Corey, A. Guzman-Perez, *Angew. Chem., Int. Ed.* **1998**, *37*, 388.
[2] T. Naota, H. Takaya, S. I. Murahashi, *Chem. Rev.* **1998**, *98*, 2599.
[3] L. Tonks, J. M. J. Williams, *J. Chem. Soc., Perkin Trans. 1* **1998**, 3637.
[4] X. Zhang, *Enantiomer* **1999**, *4*, 541.
[5] H. Tye, *J. Chem. Soc., Perkin Trans. 1* **2000**, 275.
[6] P. S. Pregosin, R. Salzmann, *Coord. Chem. Rev.* **1996**, *155*, 35.
[7] P. S. Pregosin, G. Trabesinger, *J. Chem. Soc., Dalton Trans.* **1998**, 727.
[8] P. S. Pregosin, M. Valentini, *Enantiomer* **1999**, *4*, 529.
[9] J. S. Giovannetti, C. M. Kelly, C. R. Landis, *J. Am. Chem. Soc.* **1993**, *115*, 4040.
[10] P. Stilbs, *Progr. Nucl. Magn. Reson. Spectrosc.* **1987**, *19*, 1.
[11] E. O. Stejskal, J. E. Tanner, *J. Chem. Phys.* **1965**, *42*, 288.
[12] B. D. Boss, E. O. Stejskal, J. D. Ferry, *J. Phys. Chem.* **1967**, *71*, 1501.
[13] P. Stilbs, *Anal. Chem.* **1981**, *53*, 2135.
[14] E. D. van Meerwall, *Adv. Polym. Sci.* **1984**, *54*, 1.
[15] C. B. Gorman, J. C. Smith, M. W. Hager, B. L. Parkhurst, H. Sierzputowska-Gracz, C. A. Haney, *J. Am. Chem. Soc.* **1999**, *121*, 9958.
[16] H. Ihre, A. Hult, E. Soderlind, *J. Am. Chem. Soc.* **1996**, *118*, 6388.
[17] G. R. Newkome, J. K. Young, G. R. Baker, R. L. Potter, L. Audoly, D. Cooper, C. D. Weis, K. Morris, C. S. Johnson, *Macromolecules* **1993**, *26*, 2394.
[18] I. B. Rietveld, D. Bedeaux, *Macromolecules* **2000**, *33*, 7912.
[19] R. C. van Duijvenbode, I. B. Rietveld, G. J. M. Koper, *Langmuir* **2000**, *16*, 7720.
[20] J. K. Young, G. R. Baker, G. R. Newkome, K. F. Morris, C. S. Johnson, *Macromolecules* **1994**, *27*, 3464.
[21] W. J. Chien, S. F. Cheng, D. K. Chang, *Anal. Biochem.* **1998**, *264*, 211.
[22] M. L. Liu, H. C. Toms, G. E. Hawkes, J. K. Nicholson, J. C. Lindon, *J. Biomol. NMR* **1999**, *13*, 25.
[23] S. Park, M. E. Johnson, L. W. M. Fung, *FEBS Lett.* **2000**, *485*, 81.
[24] S. G. Yao, G. J. Howlett, R. S. Norton, *J. Biomol. NMR* **2000**, *16*, 109.
[25] J. Kärger, H. Pfeifer, W. Heink, *Adv. Magn. Reson.* **1988**, *12*, 1.
[26] G. H. Sorland, D. Aksnes, L. Gjerdaker, *J. Magn. Reson.* **1999**, *137*, 397.
[27] S. Beck, A. Geyer, H. H. Brintzinger, *Chem. Commun.* **1999**, 2477.
[28] B. Olenyuk, M. D. Levin, J. A. Whiteford, J. E. Shield, P. J. Stang, *J. Am. Chem. Soc.* **1999**, *121*, 10434.
[29] C. Zuccaccia, G. Bellachioma, G. Cardaci, A. Macchioni, *Organometallics* **2000**, *19*, 4663.
[30] M. Valentini, P. S. Pregosin, H. Rüegger, *J. Chem. Soc., Dalton Trans.* **2000**, 4507.
[31] M. Valentini, P. S. Pregosin, H. Rüegger, *Organometallics* **2000**, *19*, 2551.
[32] O. Mayzel, Y. Cohen, *J. Chem. Soc., Chem. Commun.* **1994**, 1901.
[33] R. E. Hoffman, E. Shabtai, M. Rabinovitz, V. S. Iyer, K. Mullen, A. K. Rai, E. Bayrd, L. T. Scott, *J. Chem. Soc., Perkin Trans. 2* **1998**, 1659.
[34] Q. Jiang, H. Rüegger, L. M. Venanzi, *Inorg. Chim. Acta* **1999**, *290*, 64; R. M. Stoop, S. Bachman, M. Valentini, A. Mezzetti, *Organometallics* **2000**, *19*, 4117.
[35] A. Pichota, P. S. Pregosin, M. Valentini, M. Wörle, D. Seebach, *Angew. Chem., Int. Ed.* **2000**, *39*, 153.
[36] R. Colton, A. D'Agostino, J. C. Traeger, *Mass Spectrom. Rev.* **1995**, *14*, 79.
[37] G. L. Beyer, in 'Physical Methods of Chemistry', Ed. A. Weissberger, B. W. Rossiter, Wiley-Interscience, New York, 1971, Vol. 1, pp. 127–203.
[38] S. S. Pochapsky, H. Mo, T. C. Pochapsky, *J. Chem. Soc., Chem. Commun.* **1995**, 2513.
[39] C. S. Johnson in 'Encyclopedia of NMR Spectroscopy', Wiley-Interscience, New York, 1996.
[40] G. Balimann, H. Motschi, P. S. Pregosin, *Inorg. Chim. Acta* **1977**, *23*, 191.
[41] C. Köllner, B. Pugin, A. Togni, *J. Am. Chem. Soc.* **1998**, *120*, 10274.
[42] C. J. den Reijer, M. Wörle, P. S. Pregosin, *Organometallics* **2000**, *19*, 309.
[43] A. Chandra, B. Bagchi, *J. Chem. Phys.* **2000**, *113*, 3226.
[44] H. Falkenhagen, *Z. Phys.* **1931**, *32*, 745.
[45] D. Seebach, G. Jaeschke, A. Pichota, L. Audergon, *Helv. Chim. Acta* **1997**, *80*, 2515.
[46] T. J. Geldbach, P. S. Pregosin, A. Albinati, *Organometallics* **2001**, *20*, 1932.
[47] P. Schurtenberger, M. E. Newman in 'Environmental Particles', Ed. J. Buffle, H. P. van Leeuwen, Lewis, Boca Raton, 1993; Vol. 2, p. 37.
[48] Y. Chen, M. Valentini, P. S. Pregosin, A. Albinati, *Inorg. Chim. Acta*, submitted.

[49] D. Drago, P. S. Pregosin, *J. Chem. Soc., Dalton Trans.* **2000**, 3191.
[50] 'Handbook of Chemistry and Physics', 71st edn., Ed. D. R. Lide, CRC Press, Boca Raton, 1990–1991.
[51] G. Bellachioma, G. Cardaci, A. Macchioni, G. Reichenbach, S. Terenzi, *Organometallics* **1996**, *15*, 4349.
[52] D. A. Evans, J. A. Murry, P. von Matt, R. D. Norcross, S. J. Miller, *Angew. Chem., Int. Ed*. **1995**, *34*, 798.
[53] A. Lightfoot, P. Schnider, A. Pfaltz, *Angew. Chem., Int. Ed*. **1998**, *37*, 2897.
[54] B. M. Trost, R. C. Bunt, *J. Am. Chem. Soc*. **1998**, *120*, 70.
[55] C. J. den Reijer, H. Rüegger, P. S. Pregosin, *Organometallics* **1998**, *17*, 5213.
[56] H. Ponstingl, G. Otting, *J. Biomol. NMR* **1997**, *9*, 441.
[57] G. Otting, K. Wuthrich, *Q. Rev. Biophys.* **1990**, *23*, 39.
[58] P. S. Pregosin, R. Rüedi, *J. Organomet. Chem*. **1984**, *273*, 401.
[59] H. J. W. Tyrrell, K. R. Harris in 'Diffusion in Liquids', Ed. H. J. W. Tyrrell, K. R. Harris, Butterworths, London, 1984.
[60] L. L. Martin, R. A. Jacobsen, *Inorg. Chem*. **1971**, *10*, 1795.
[61] I. Y. Guzman-Jimenez, K. H. Whitmire, *Acta Crystallogr*. **1999**, *C55*, IUC9900028.
[62] A. J. M. Caffyn, S. G. Feng, A. Dierdorf, A. S. Gamble, P. A. Eldredge, M. R. Vossen, P. S. White, J. L. Templeton, *Organometallics* **1991**, *10*, 2842.
[63] D. Drago, P. S. Pregosin, M. Tschoerner, A. Albinati, *J. Chem. Soc., Dalton Trans.* **1999**, 2279.
[64] M. Tschoerner, P. S. Pregosin, A. Albinati, unpublished results.
[65] K. Selvakumar, M. Valentini, M. Wörle, P. S. Pregosin, *Organometallics* **1999**, *18*, 1207.
[66] G. Schultz, N. Y. Subbotina, C. M. Jensen, J. A. Golen, I. Hargittai, *Inorg. Chim. Acta* **1992**, *191*, 85.
[67] G. Ferguson, R. McCrindle, A. J. McAlees, M. Perez, *Acta Crystallogr.* **1982**, *B38*, 2679.

Received March 3, 2001